Supplement to "Stratospheric aerosol forcing for CMIP7 – Part 3: comparison with CMIP6 and evaluation using complementary datasets"

Man Mei Chim[1], Dominik Stiller[2], Elisa Ziegler[3], Thomas J. Aubry[4,5], Lucas Boissel[6,7,8], Sebastien Guillet[9], Brennan Rodgers[10], Matthew Toohey[10], Christine Pohl[11,12], and Alexei Rozanov[11]

[1]Department of Mathematics and Statistics, University of Exeter, Exeter, United Kingdom
[2]Department of Atmospheric and Climate Science, University of Washington, Seattle, WA, USA
[3]Department of Geosciences, University of Tübingen, Tübingen, Germany
[4]Department of Earth Sciences, University of Oxford, Oxford, United Kingdom
[5]Department of Earth and Environmental Sciences, University of Exeter, Penryn, Cornwall, United Kingdom
[6]Université Paris Cité, Paris, France
[7]Pôle de recherche pour l'organisation et la diffusion de l'information géographique (PRODIG), Paris, France
[8]Laboratoire de Géographie Physique: Environnements Quaternaires et Actuels (LGP), Thiais, France
[9]Climate Change Impacts and Risks in the Anthropocene (C-CIA), Institute for Environmental Sciences, University of Geneva, Geneva, Switzerland
[10]Institute of Space and Atmospheric Studies, University of Saskatchewan, Saskatoon, Canada
[11]Institute of Environmental Physics, University of Bremen, Bremen, Germany
[12]Now at the Department of Physics, Lund University, Lund, Sweden

Correspondence: Man Mei Chim (m.m.chim@exeter.ac.uk), Dominik Stiller (dstiller@uw.edu), and Elisa Ziegler (elisa.ziegler@uni-tuebingen.de)

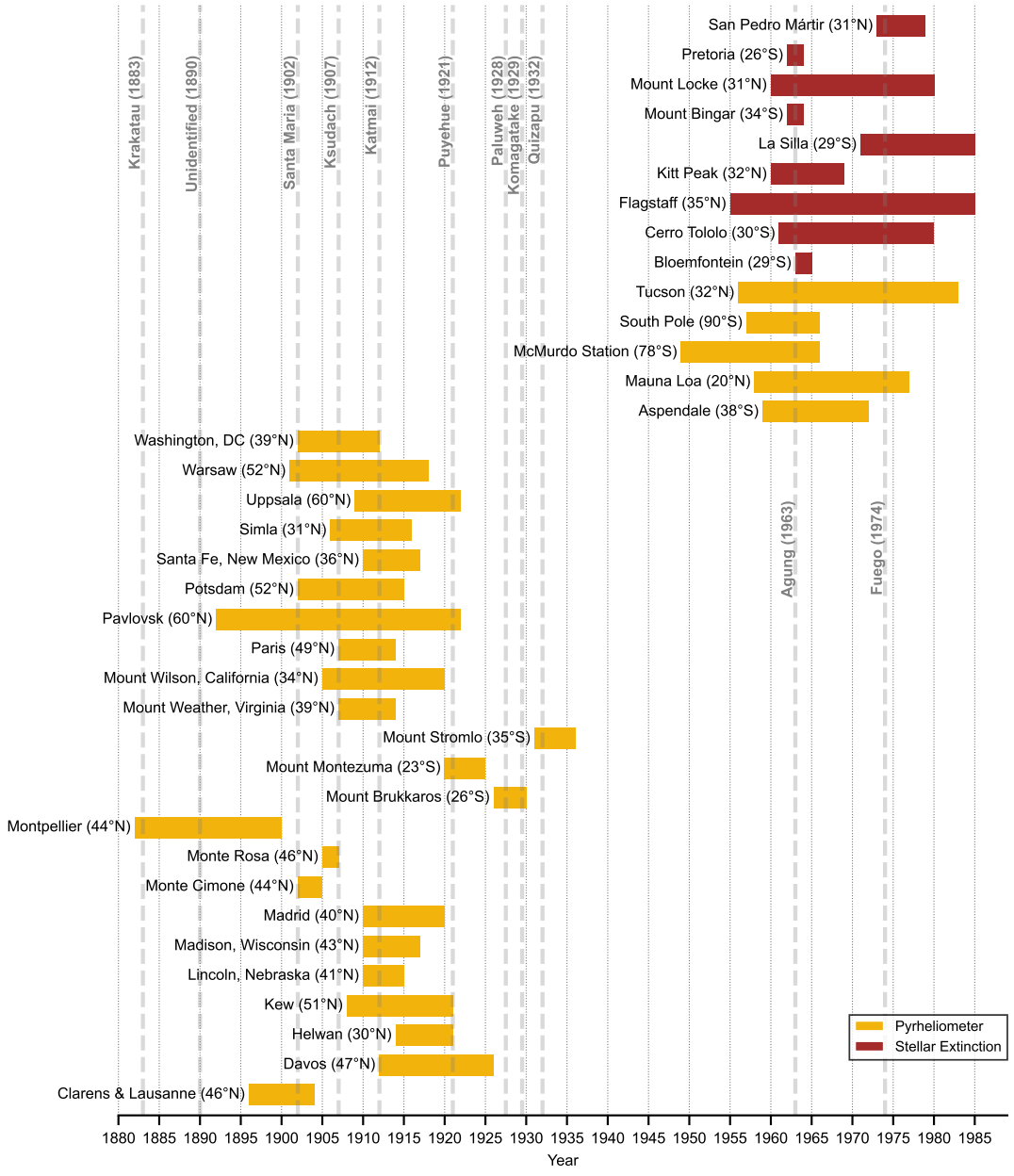

Figure S1. Time coverage of pyrheliometer stations from Stothers (1996, 2001) and stellar extinction sites from Stothers (2001). The grey vertical lines denote the major volcanic eruptions with pyrheliometric optical depth reported by Stothers (1996, 2001).

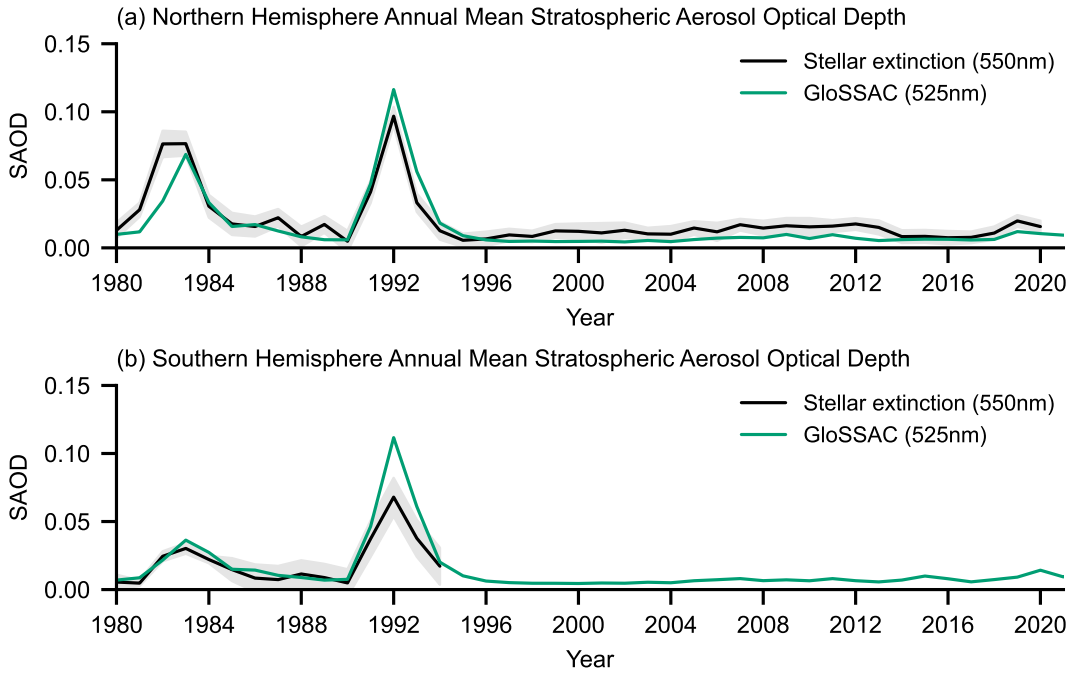

Figure S2. (a) Northern Hemisphere and (b) Southern Hemisphere annual-mean stratospheric aerosol optical depth from stellar extinction measurements at 550 nm (Rodgers and Toohey, 2026), and from GloSSAC at 525 nm (Kovilakam et al., 2020).

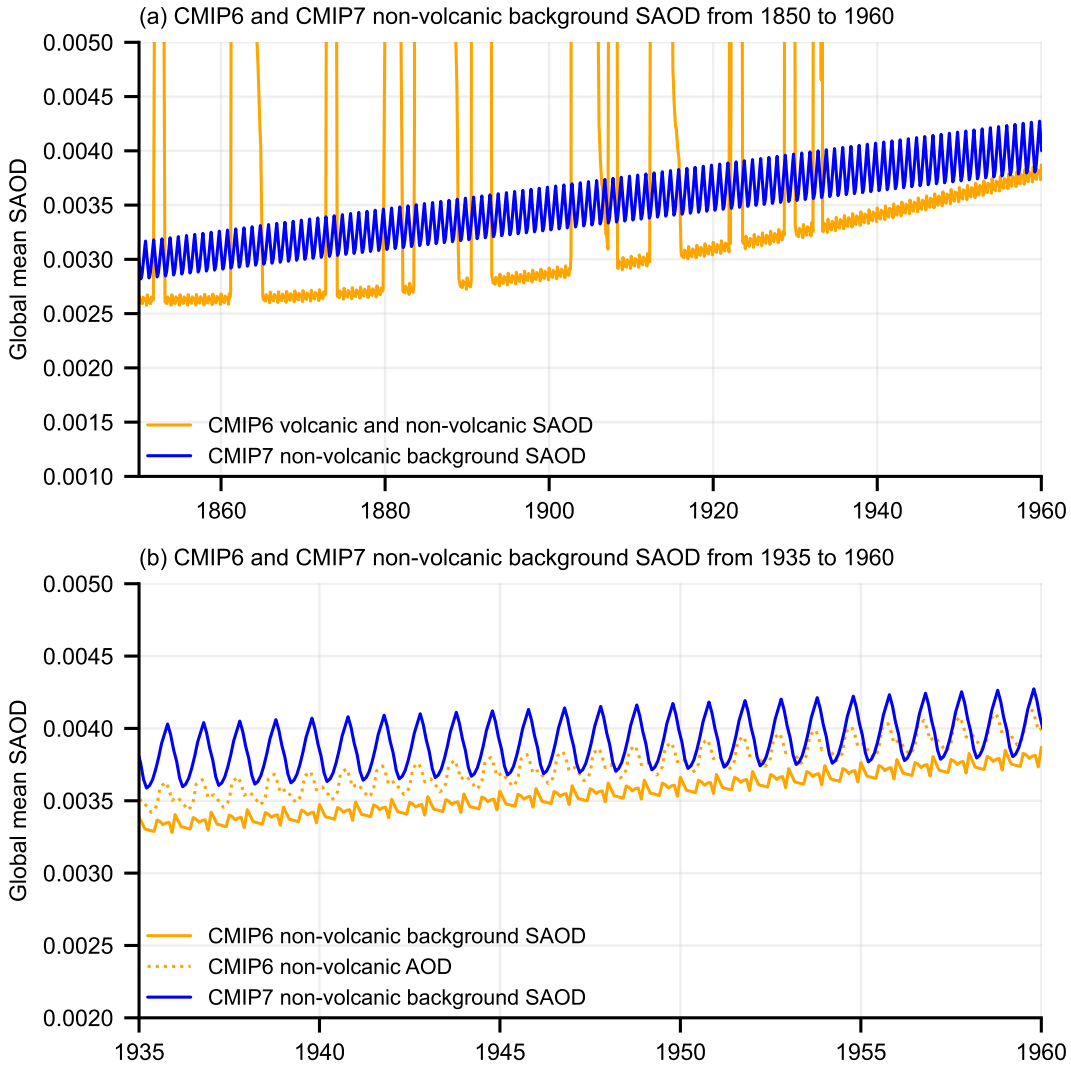

Figure S3. (a) Global-mean stratospheric aerosol optical depth from 1850 to 1960 for CMIP6 (volcanic and non-volcanic background) and CMIP7 (non-volcanic background), (b) Global-mean stratospheric aerosol optical depth for CMIP6 and CMIP7 during the volcanically quiescent period from 1935 to 1960. The CMIP6 non-volcanic AOD in (b) is the same as the CMIP6 non-volcanic background SAOD, but integrated over the whole atmosphere without the troposphere mask.

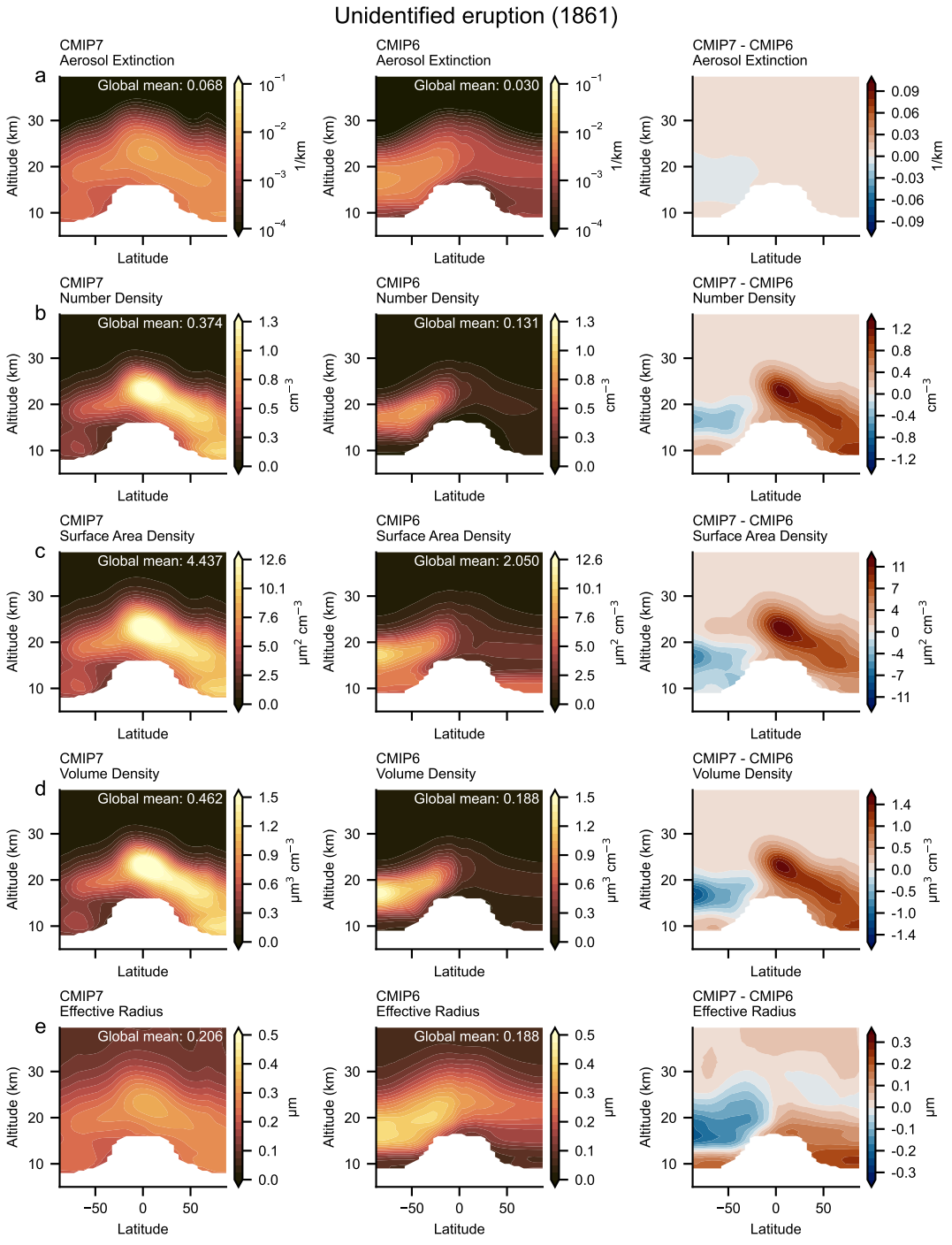

Figure S4. Zonal-mean (a) extinction coefficient, (b) number density, (c) surface area density, (d) volume density, and (e) effective radius, averaged over 12 months following the 1861 Unidentified eruption. (Left) CMIP7, (Middle) CMIP6, and (Right) Difference between CMIP7 and CMIP6. The global-mean values are calculated as the 12-month-mean following the eruption; in (a), they denote the stratospheric aerosol optical depth.

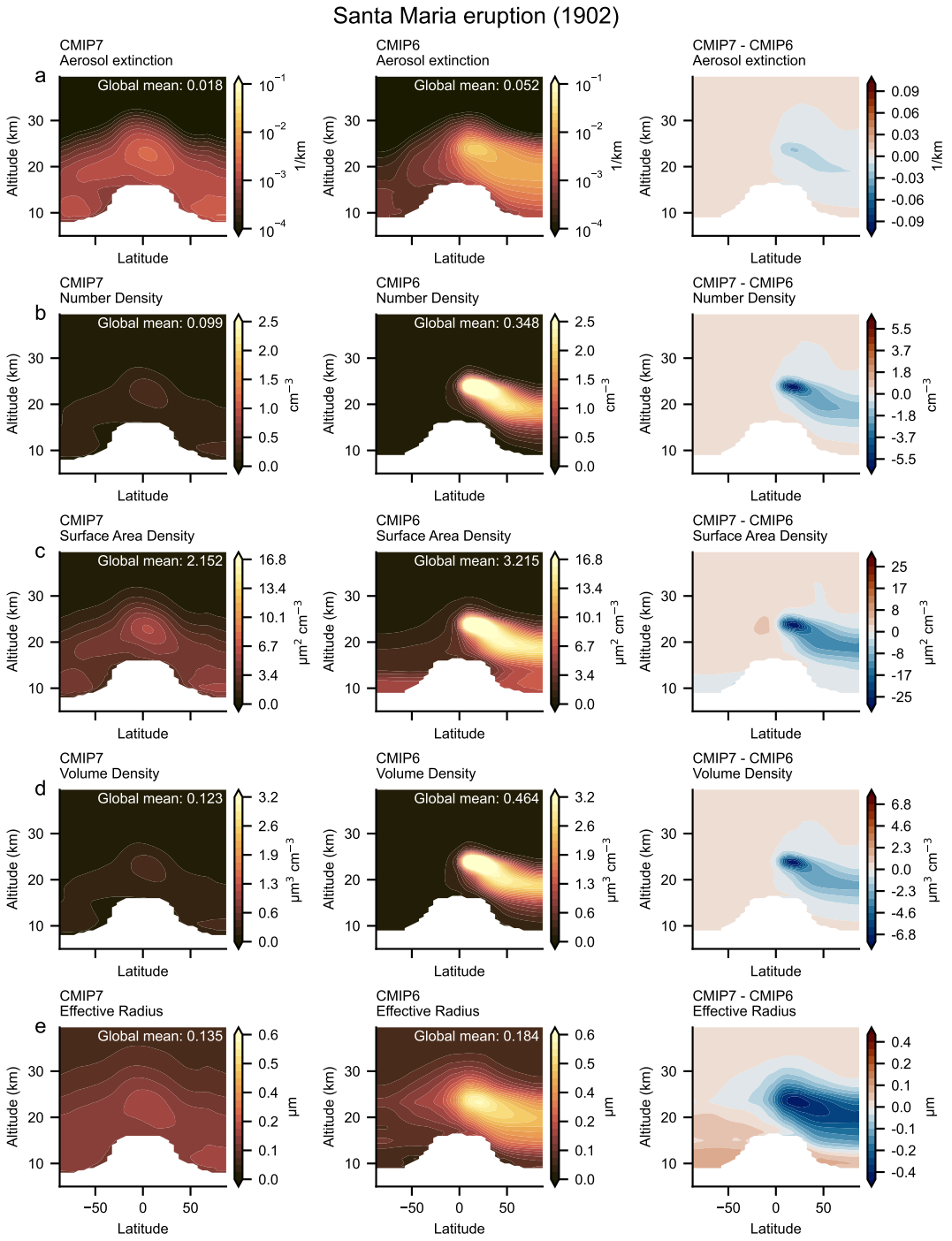

Figure S5. Same as Figure S4 but for the 1902 Santa María eruption.

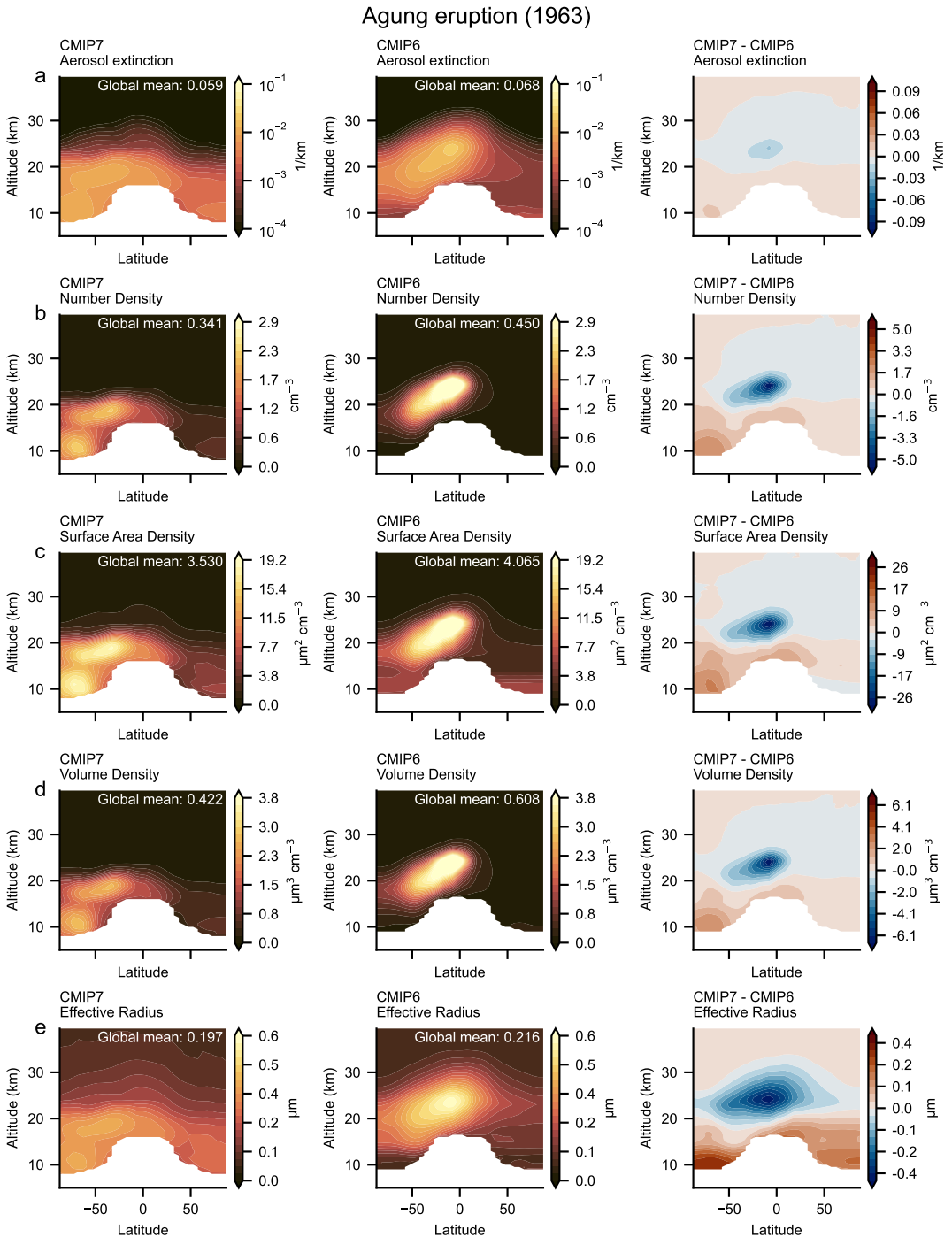

Figure S6. Same as Figure S4 but for the 1963 Agung eruption.

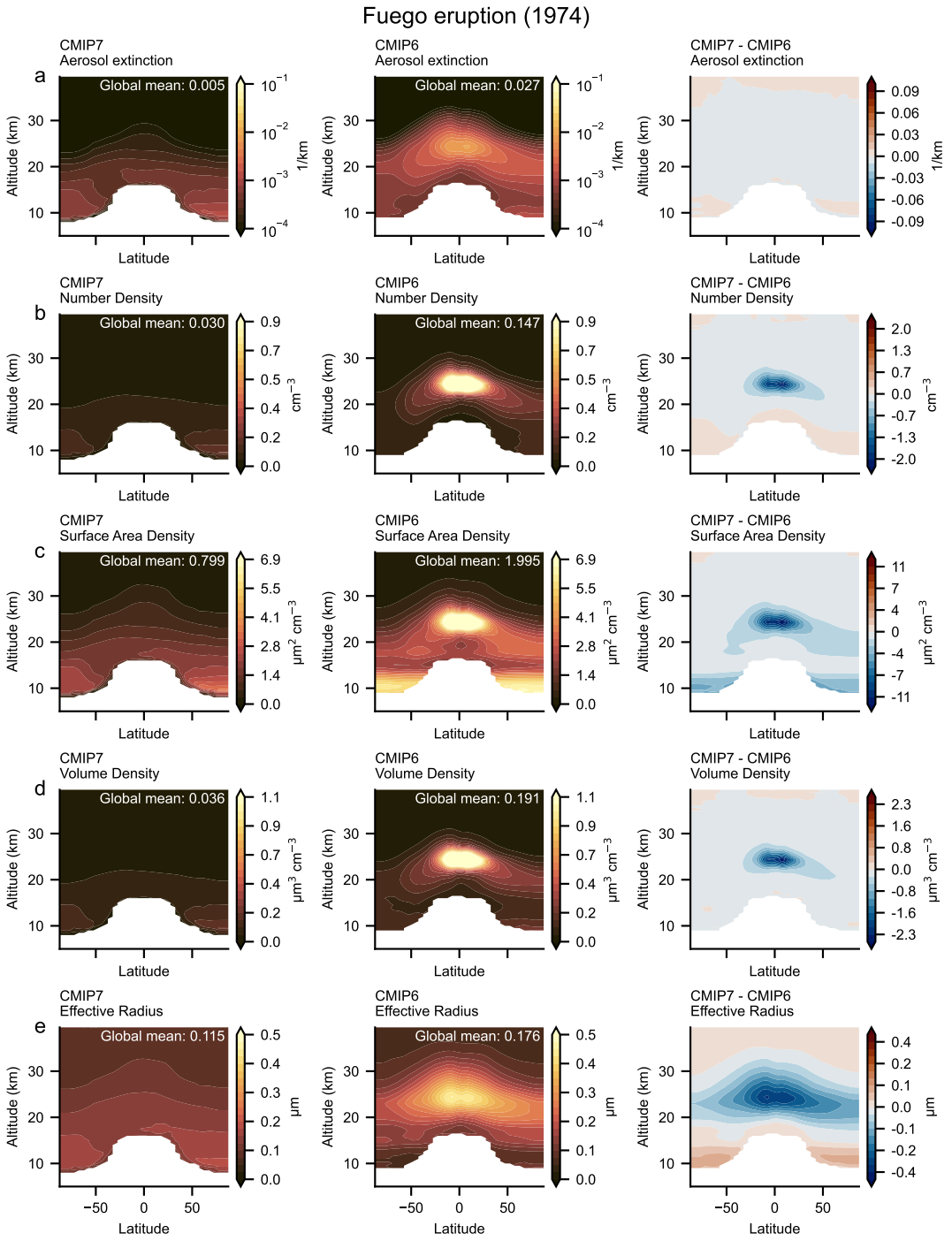

Figure S7. Same as Figure S4 but for the 1974 Fuego eruption.

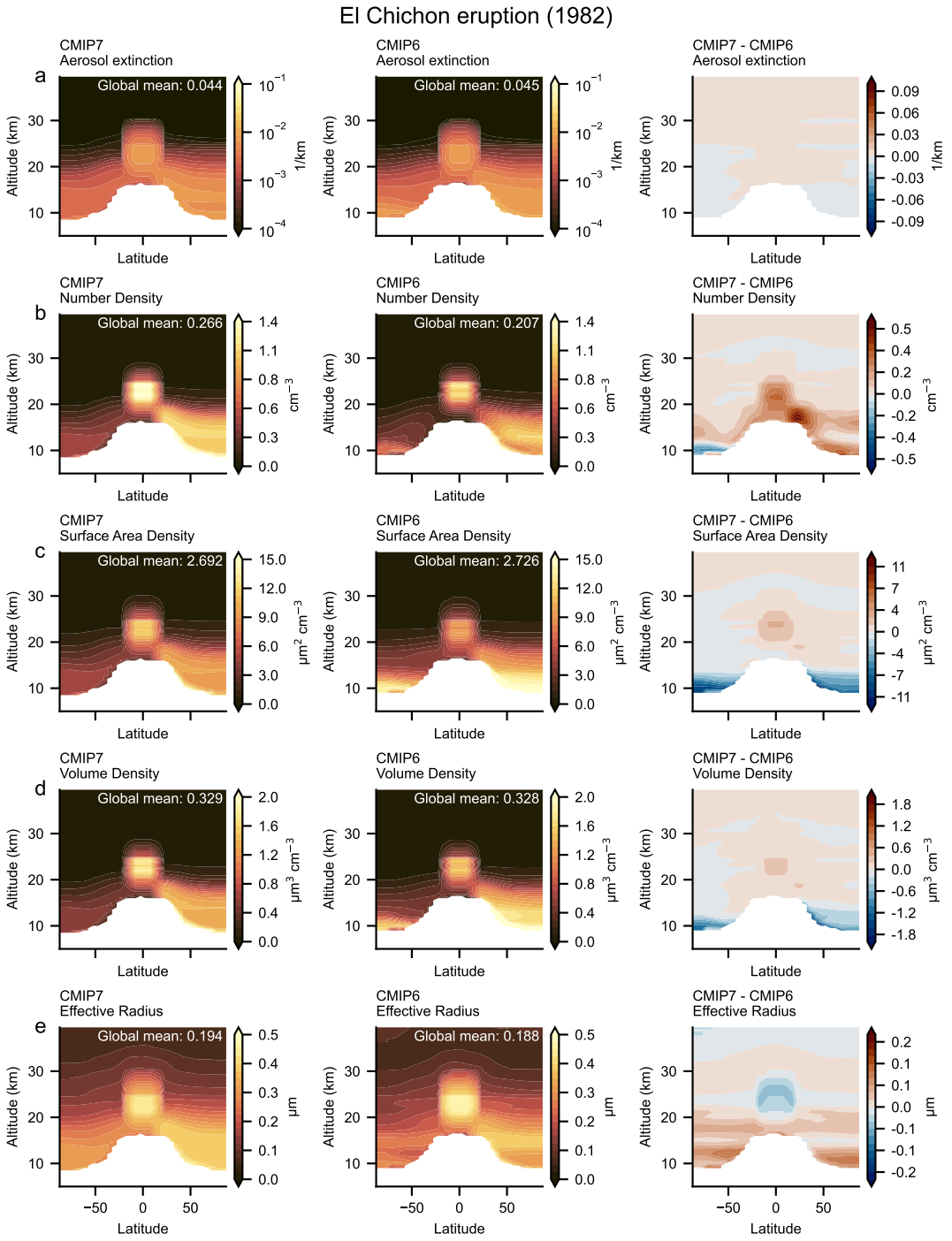

Figure S8. Same as Figure S4 but for the 1982 El Chichón eruption.

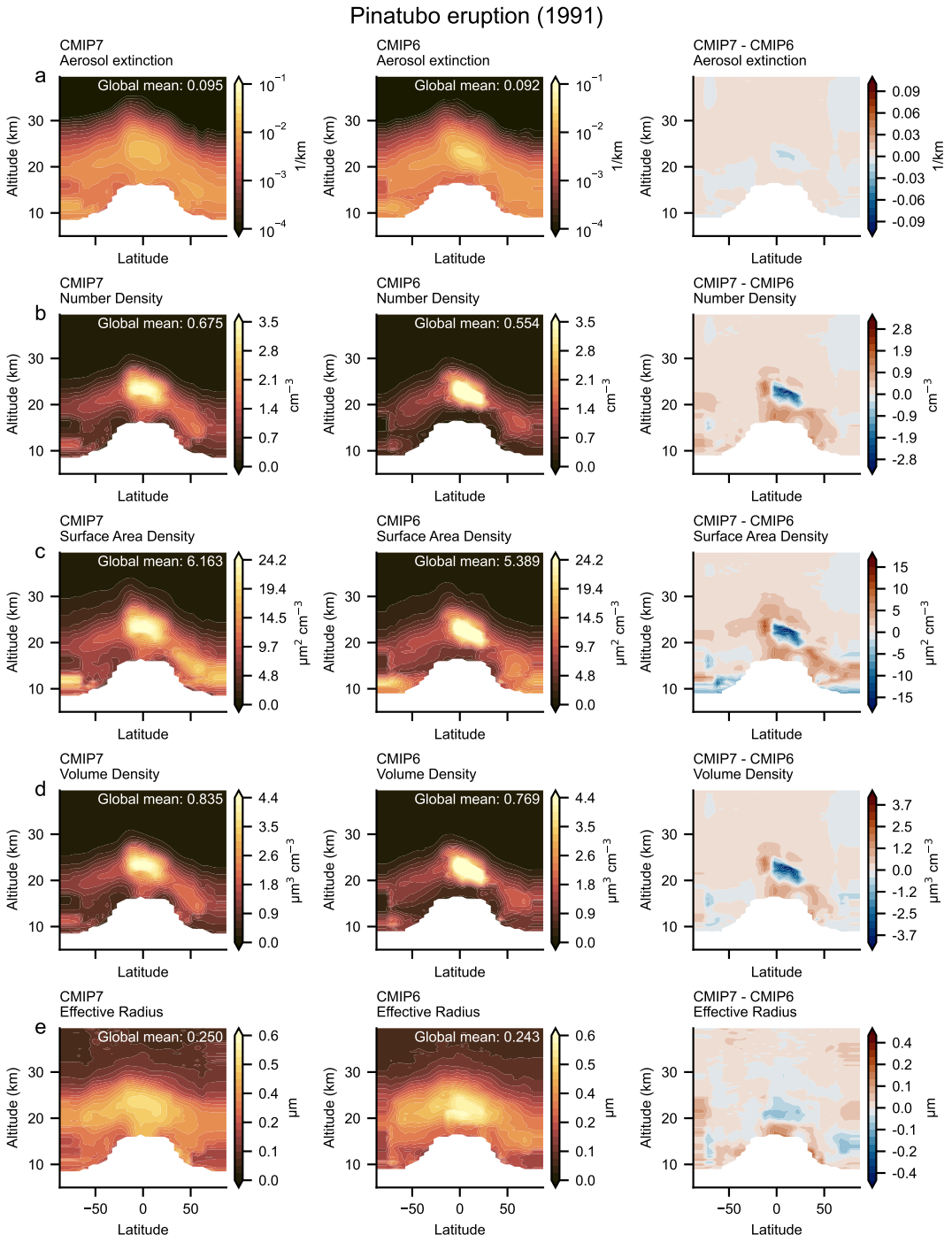

Figure S9. Same as Figure S4 but for the 1991 Pinatubo eruption.

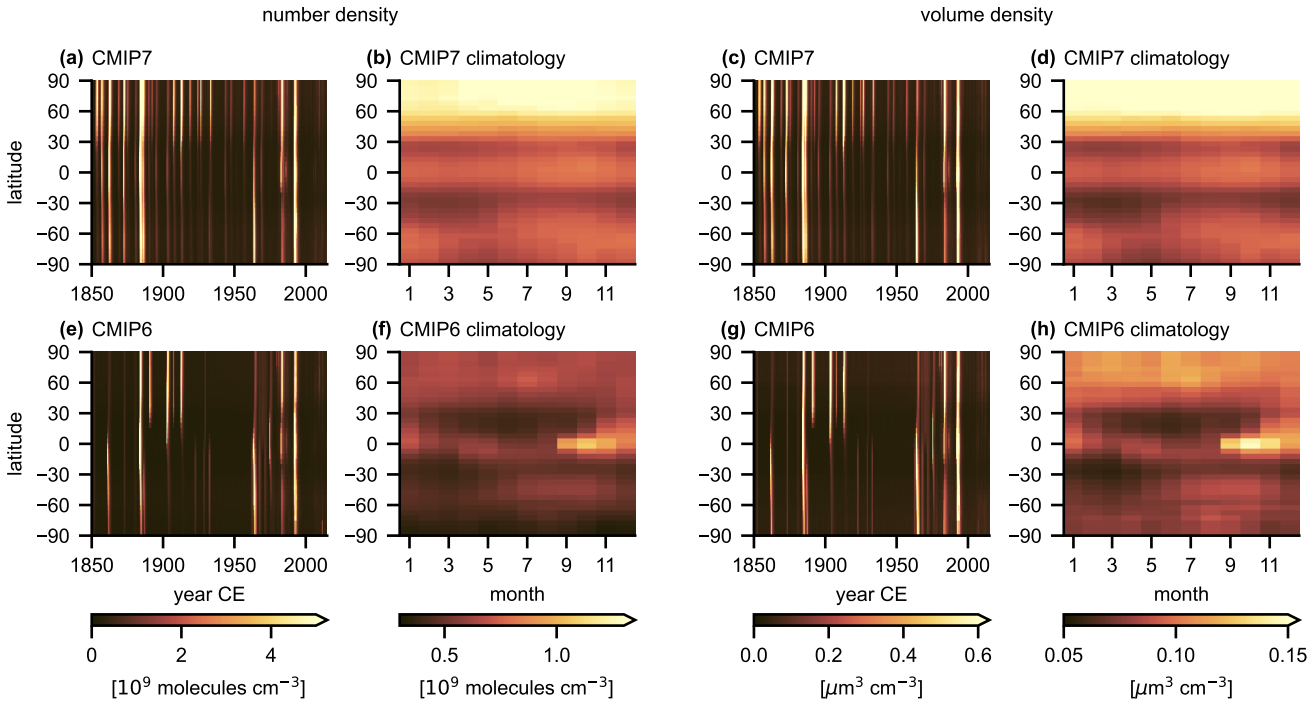

Figure S10. Number density (left-hand side) and volume density (right-hand side) in CMIP7 (top row) and CMIP6 (bottom row). (a, c, e, g) Latitudinal change with time from 1850 to 2014 CE averaged along altitude. (b, d, f, h) Latitudinal patterns in the climatologies per month.

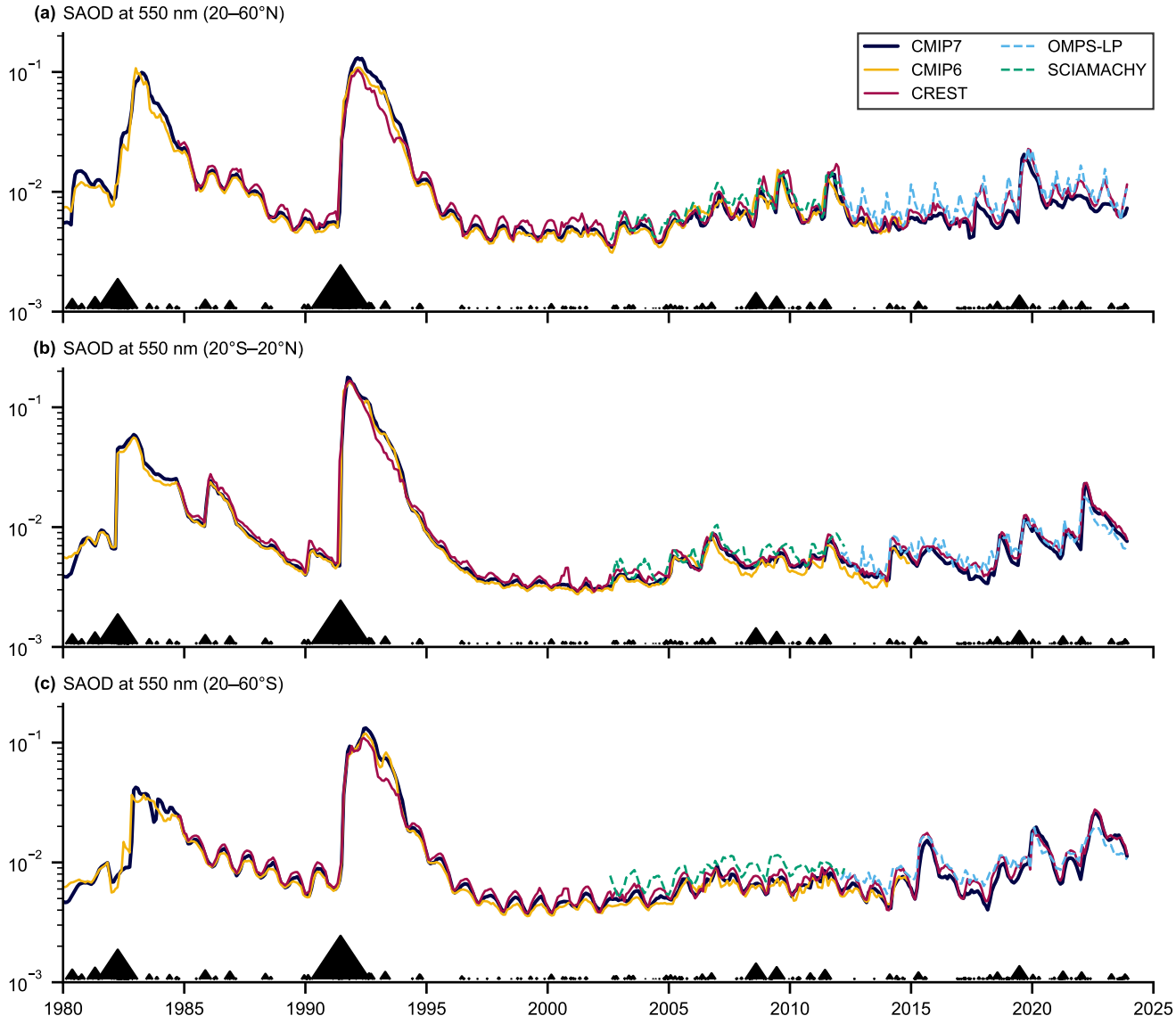

Figure S11. Stratospheric aerosol optical depth in CMIP7, CMIP6, and other satellite datasets at 550 nm. CMIP7 and CMIP6 are based on GloSSAC, which does not include OMPS-LP and SCIAMACHY data. CREST is a merged dataset that includes mostly the same satellite data as GloSSAC, and additionally OMPS-LP, SCIAMACHY, and GOMOS data. CREST (750 nm; Sofieva et al., 2024), OMPS-LP (869 nm; retrieval by Rozanov et al., 2024), and SCIAMACHY (525 nm; retrieval by Pohl et al., 2024) were converted to 550 nm using the Ångström formula with a time-varying zonal-mean α derived from the 525 nm and 1020 nm extinction of CMIP7. The monthly climatological tropopause from CMIP7 is applied to satellite datasets. Black triangles indicate volcanic eruptions in CMIP7 (Aubry et al., 2026), scaled by their volcanic stratospheric sulfur injection.

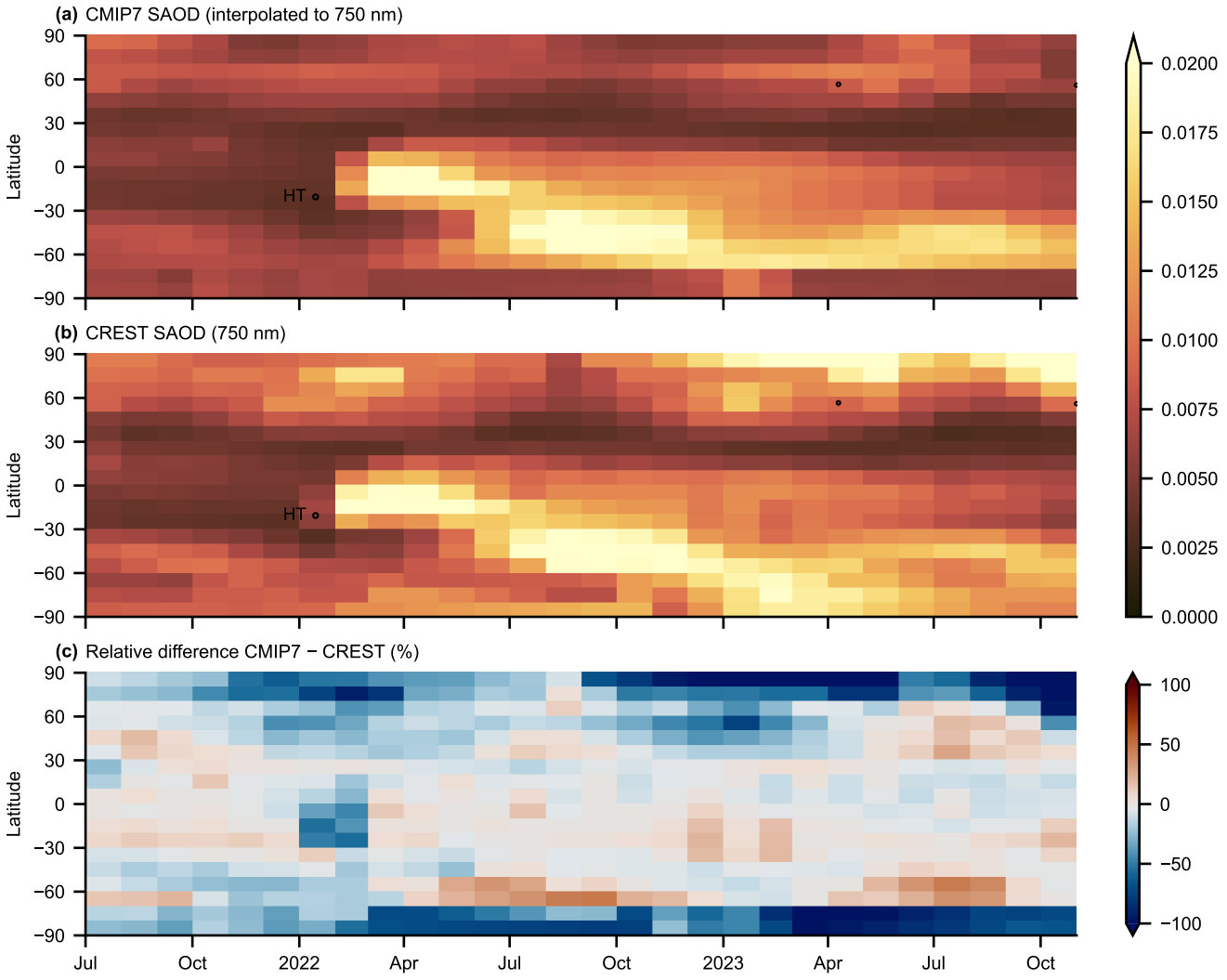

Figure S12. Stratospheric aerosol optical depth in CMIP7 and CREST satellite observations at 750 nm for the Hunga Tonga–Hunga Ha'apai (HT) eruption. The CMIP7 5° data were binned to the CREST 10° latitude grid. The monthly climatological tropopause from CMIP7 is applied to CREST. Black circles indicate volcanic eruptions exceeding 0.5 Tg SO_2 scaled by injected SO_2 mass.

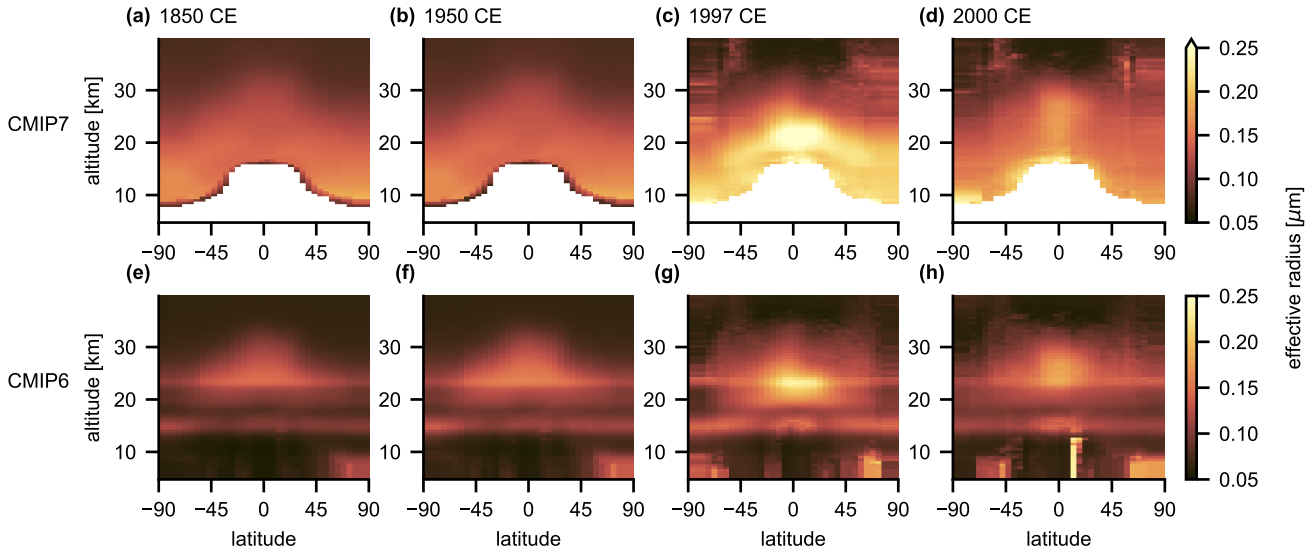

Figure S13. Effective aerosol radius in CMIP7 (top row) and CMIP6 (bottom row) during volcanically quiescent years in the pre-satellite and satellite era.

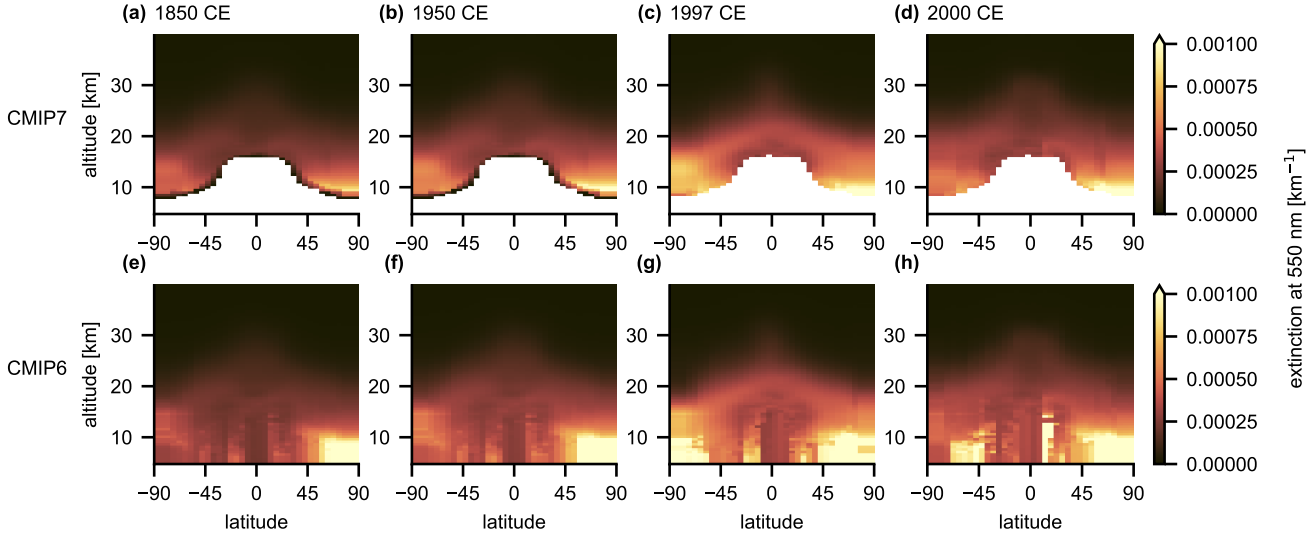

Figure S14. Extinction coefficient at 550 nm in CMIP7 (top row) and CMIP6 (bottom row) during volcanically quiescent years in the pre-satellite and satellite era.

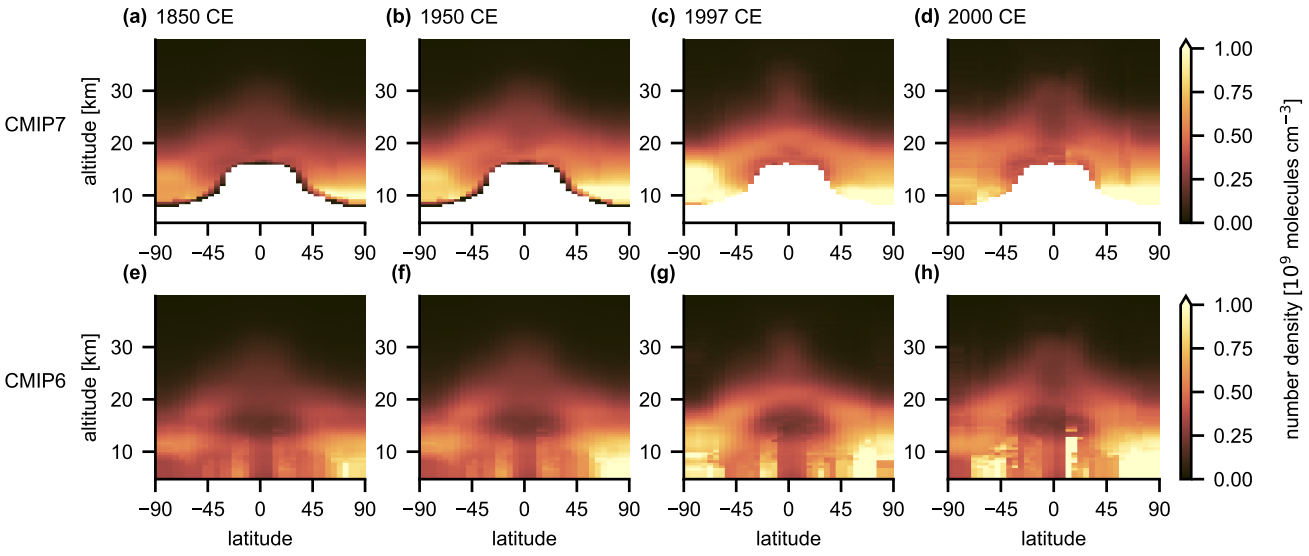

Figure S15. Number density in CMIP7 (top row) and CMIP6 (bottom row) during volcanically quiescent years in the pre-satellite and satellite era.

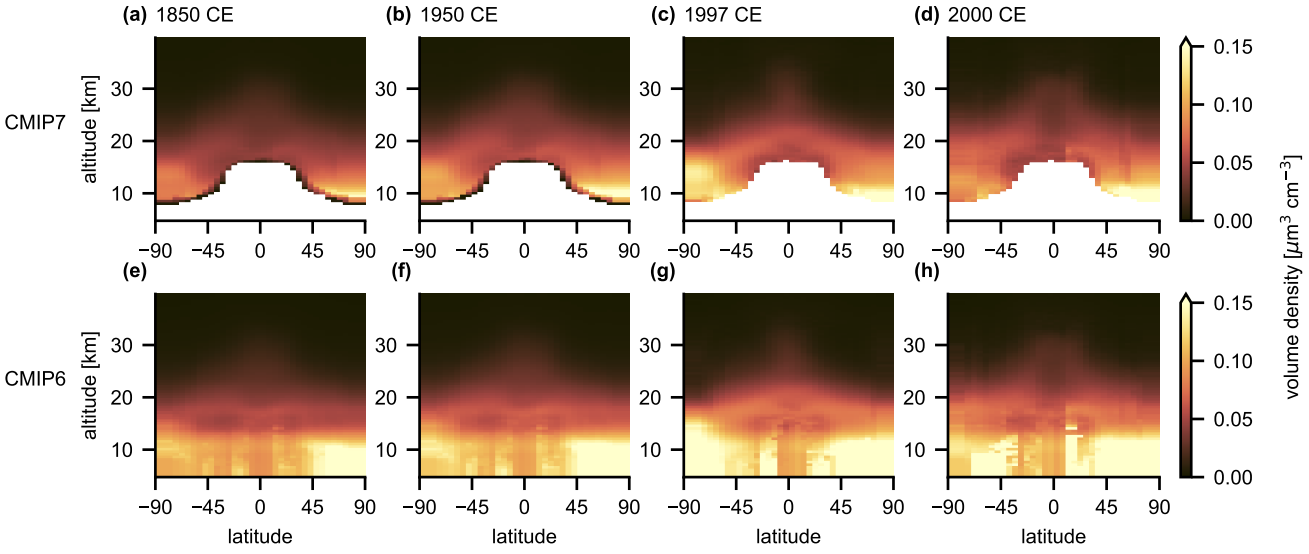

Figure S16. Volume density in CMIP7 (top row) and CMIP6 (bottom row) during volcanically quiescent years in the pre-satellite and satellite era.

References

Aubry, T. J., Toohey, M., Khanal, S., Chim, M. M., Verkerk, M., Johnson, B., Schmidt, A., Kovilakam, M., Sigl, M., Nicholls, Z., Thomason, L., Naik, V., Rieger, L., Stiller, D., Ziegler, E., Durack, P., and Smith, I. H.: Stratospheric aerosol forcing for CMIP7 – Part 1: optical properties for pre-industrial, historical, and scenario simulations, Geoscientific Model Development, 19, 3725–3756, https://doi.org/10.5194/gmd-19-3725-2026, 2026.

Kovilakam, M., Thomason, L. W., Ernest, N., Rieger, L., Bourassa, A., and Millán, L.: The Global Space-based Stratospheric Aerosol Climatology (version 2.0): 1979–2018, Earth System Science Data, 12, 2607–2634, https://doi.org/10.5194/essd-12-2607-2020, 2020.

Pohl, C., Wrana, F., Rozanov, A., Deshler, T., Malinina, E., Von Savigny, C., Rieger, L. A., Bourassa, A. E., and Burrows, J. P.: Stratospheric aerosol characteristics from SCIAMACHY limb observations: two-parameter retrieval, Atmospheric Measurement Techniques, 17, 4153–4181, https://doi.org/10.5194/amt-17-4153-2024, 2024.

Rodgers, B. and Toohey, M.: Estimation of SAOD from measurements of Stellar Attenuation 1955-2020, https://doi.org/10.5281/zenodo.18488959, 2026.

Rozanov, A., Pohl, C., Arosio, C., Bourassa, A., Bramstedt, K., Malinina, E., Rieger, L., and Burrows, J. P.: Retrieval of stratospheric aerosol extinction coefficients from sun-normalized Ozone Mapper and Profiler Suite Limb Profiler (OMPS-LP) measurements, Atmospheric Measurement Techniques, 17, 6677–6695, https://doi.org/10.5194/amt-17-6677-2024, 2024.

Sofieva, V. F., Rozanov, A., Szelag, M., Burrows, J. P., Retscher, C., Damadeo, R., Degenstein, D., Rieger, L. A., and Bourassa, A.: CREST: a Climate Data Record of Stratospheric Aerosols, Earth System Science Data, 16, 5227–5241, https://doi.org/10.5194/essd-16-5227-2024, 2024.

Stothers, R. B.: Major optical depth perturbations to the stratosphere from volcanic eruptions: Pyrheliometric period, 1881–1960, Journal of Geophysical Research: Atmospheres, 101, 3901–3920, https://doi.org/10.1029/95JD03237, 1996.

Stothers, R. B.: Major optical depth perturbations to the stratosphere from volcanic eruptions: Stellar extinction period, 1961–1978, Journal of Geophysical Research: Atmospheres, 106, 2993–3003, https://doi.org/10.1029/2000JD900652, 2001.